Research Article

Production of CO-rich Hydrogen Gas from Methane Dry Reforming over Co/CeO₂ Catalyst

Bamidele V. Ayodele, Maksudur R. Khan, Chin Kui Cheng*

[1]Faculty of Chemical & Natural Resources Engineering, Universiti Malaysia Pahang, Lebuhraya Tun Razak, 26300 Gambang Kuantan, Pahang, Malaysia

Abstract

Production of CO-rich hydrogen gas from methane dry reforming was investigated over CeO₂-supported Co catalyst. The catalyst was synthesized by wet impregnation and subsequently characterized by field emission scanning electron microscope (FESEM), energy-dispersive X-ray spectroscopy (EDX), liquid N₂ adsorption-desorption, X-ray diffraction (XRD), Fourier transform infrared spectroscopy (FTIR) and thermogravimetric analysis (TGA) for the structure, surface and thermal properties. The catalytic activity test of the Co/CeO₂ was investigated between 923-1023 K under reaction conditions in a stainless steel fixed bed reactor. The composition of the products (CO and H₂) from the methane dry reforming reaction was measured by gas chromatography (GC) coupled with thermal conductivity detector (TCD). The effects of feed ratios and reaction temperatures were investigated on the catalytic activity toward product selectivity, yield, and syngas ratio. Significantly, the selectivity and yield of both H₂ and CO increases with feed ratio and temperature. However, the catalyst shows higher activity towards CO selectivity. The highest H₂ and CO selectivity of 19.56% and 20.95% respectively were obtained at 1023 K while the highest yield of 41.98% and 38.05% were recorded for H₂ and CO under the same condition. Copyright © 2016 BCREC GROUP. All rights reserved

Keywords: Methane dry reforming; hydrogen; syngas; Co/CeO₂ Catalyst; CO-rich Hydrogen Gas

1. Introduction

In the past three decades, there has been an increasing trend in the global hydrogen production [1] due to its wide applications as an energy carrier [2]. Hydrogen gas is widely used for different industrial processes such as fertilizer and methanol production, crude oil refining, metal refining, food processing and electronics manufacturing [3-4]. Recently, attention of researchers have shifted to the use of hydrogen as fuel source due to its high calorific value [5-6]. This has resulted into breakthrough in the application of hydrogen fuel cells as source of energy for propelling spacecraft, powering remote weather stations and submarines as well as electric vehicles [7-8].

* Corresponding Author.
  E-mail: chinkui@ump.edu.my (C.K. Cheng),
  bamidele.ayodele@uniben.edu (B.V. Ayodele)
  Tel: +60-9-5492896, Fax: +60-9-5492889

The mixture of H_2 and CO otherwise known as synthesis (syngas) can also be employed as chemical intermediate for the production of synthetic fuel either through Fischer-Tropsch synthesis or Mobil Methanol-To-Gasoline process [9-10].

Hydrogen gas can be produced using different technologies such as natural gas reforming [11], gasification (biomass or coal) [12] and through biological process [13]. Coal gasification is one of the early technologies employed in the production of H_2 and it is being used by SASOL for commercial production of hydrogen [14]. However, the process has raised a lot of environmental concerns due to CO_2 and carcinogen emissions that often come with the process [15]. Presently, about 50% of the world consumption of hydrogen is commercially produced from natural gas reforming otherwise known as steam reforming of methane (Equation (1)) [16]. Besides steam methane reforming, hydrogen can also be produced from partial oxidation of methane [17] (Equation (2)) which involves the partial combustion of methane in air. These two processes (steam methane reforming and partial oxidation) produce syngas which can further be converted to higher content of hydrogen through water gas shift reaction represented in Equation (3).

$$CH_4 + H_2O \leftrightarrow CO + 3H_2$$
$$\Delta H_r^o = 206 \ kJmol^{-1}$$
(1)

$$CH_4 + \frac{3}{2}O_2 \rightarrow CO + 2H_2$$
$$\Delta H_r^o = 165 \ kJmol^{-1}$$
(2)

$$CO + H_2O \leftrightarrow CO_2 + H_2$$
$$\Delta H_r^o = -41.2 \ kJmol^{-1}$$
(3)
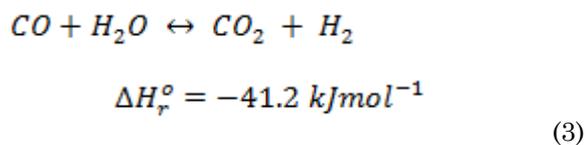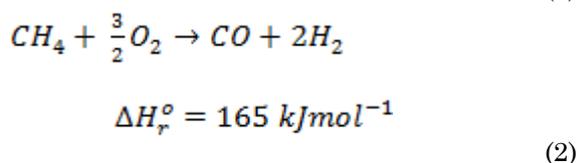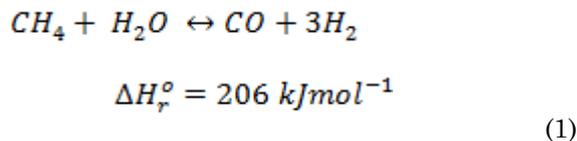
Although, methane steam reforming and coal gasification are well established technologies for H_2 production, nevertheless, the process does not mitigate CO_2 emission into the atmosphere [18]. Moreover, catalyst deactivation from sulfur poisoning, sintering and carbon deposition are also major constraints associated with H_2 production using methane steam reforming [19].

A more environmental friendly way of producing H_2 is through the reaction of CO_2 with natural gas (methane) otherwise known as methane dry reforming (Equation (4)) [20]. Methane dry reforming has the advantage of utilizing the two principal components of greenhouse gases for H_2 or syngas production compared to gasification and steam reforming process [21]. Besides, the process produces H_2/CO ratio < 2, suitable for the production of synthetic fuel via Fischer-Tropsch synthesis [22].

$$CH_4 + CO \leftrightarrow 2CO + 2H_2$$
$$\Delta H_r^o = 247 \ kJmol^{-1}$$
(4)
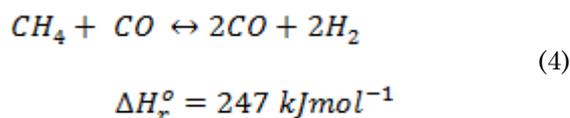
Nonetheless, the process is also prone to catalysts deactivation from sintering and carbon deposition due to the high temperature requirement of the reaction [23]. In an attempt to design and develop more stable catalysts, metal catalysts, such as: Ru, Pt, Co, Pd, Ir, dispersed on different supports (Al_2O_3, ZrO_2, SiO_2, MgO and CeO_2) have been investigated for methane dry reforming [24]. However, very few literatures have reported hydrogen production over Co/CeO_2 catalyst.

Luisetto *et al.* [25] investigated the catalytic properties of Co-Ni bimetallic catalyst supported on CeO_2 in methane dry reforming and compared the catalytic activity with CeO_2 supported Co and Ni monometallic catalysts. The findings show that the Co-Ni bimetallic catalyst displayed higher activity compared to the supported Co and Ni monometallic catalysts. Recently, Abasaeed *et al.* [26] investigated H_2 production from methane dry reforming over nano-oxides (CeO_2 and ZrO_2) supported Co catalysts. The effects of calcinations temperature ranged from 773-1173 K on the catalysts activities were evaluated. The results of the study show that the catalysts calcined at 773 and 873 K exhibited higher H_2 yield compared to those calcined at higher temperature.

In the present study, production of CO-rich H_2 from methane dry reforming over CeO_2 supported Co catalyst is reported. The CeO_2 support was synthesized by thermal decomposition of Cerium(II) nitrate hexahydrate. The main objective of this study is to investigate the catalytic activity of CeO_2 supported Co catalyst in methane dry reforming for CO-rich H_2 production.

2. Materials and Methods

2.1. Catalyst synthesis

First, the CeO_2 support was prepared by

thermal decomposition of ceriun(II) nitrate hexanitrate (99.99% purity, Sigma-Aldrich) in a furnace at 773 K for 2 hours [27]. The 20 wt% Co/CeO_2 catalyst was prepared by impregnating the CeO_2 support with aqueous solution of cobalt(III) nitrate hexanitrate (99.99% purity, Sigma-Aldrich) to produce 20 wt% Co loading. The mixture was continuously stirred for 3 hours, dried in the oven for 24 h at 393 K and then calcined at 873 K for 5 h.

2.2. Catalyst characterization

Temperature programmed calcination of the fresh catalysts was performed by Thermogravimetric analyzer (TGA) (TA instrument) in the temperature range from 298-1173 K under compressed air in order to determine the thermal stability of the catalyst. The crystallinity of the catalysts was measured by X-ray diffraction analysis (XRD). The XRD was carried out using a RIGAKU miniflex II X-ray diffractometer with Cu Kα X-ray source at wavelength (λ) of 0.154 nm radiation.

The catalysts surface morphology and the elemental composition were analyzed by field emission scanning electron microscopy (FESEM) coupled with energy dispersive X-ray (EDX) spectroscopy. Information on the textural properties of the catalyst was obtained from N_2 adsorption-desorption isotherms data by Thermo Scientific Surfer analyzer. The sample was degassed at 523 K for 4 h prior to the
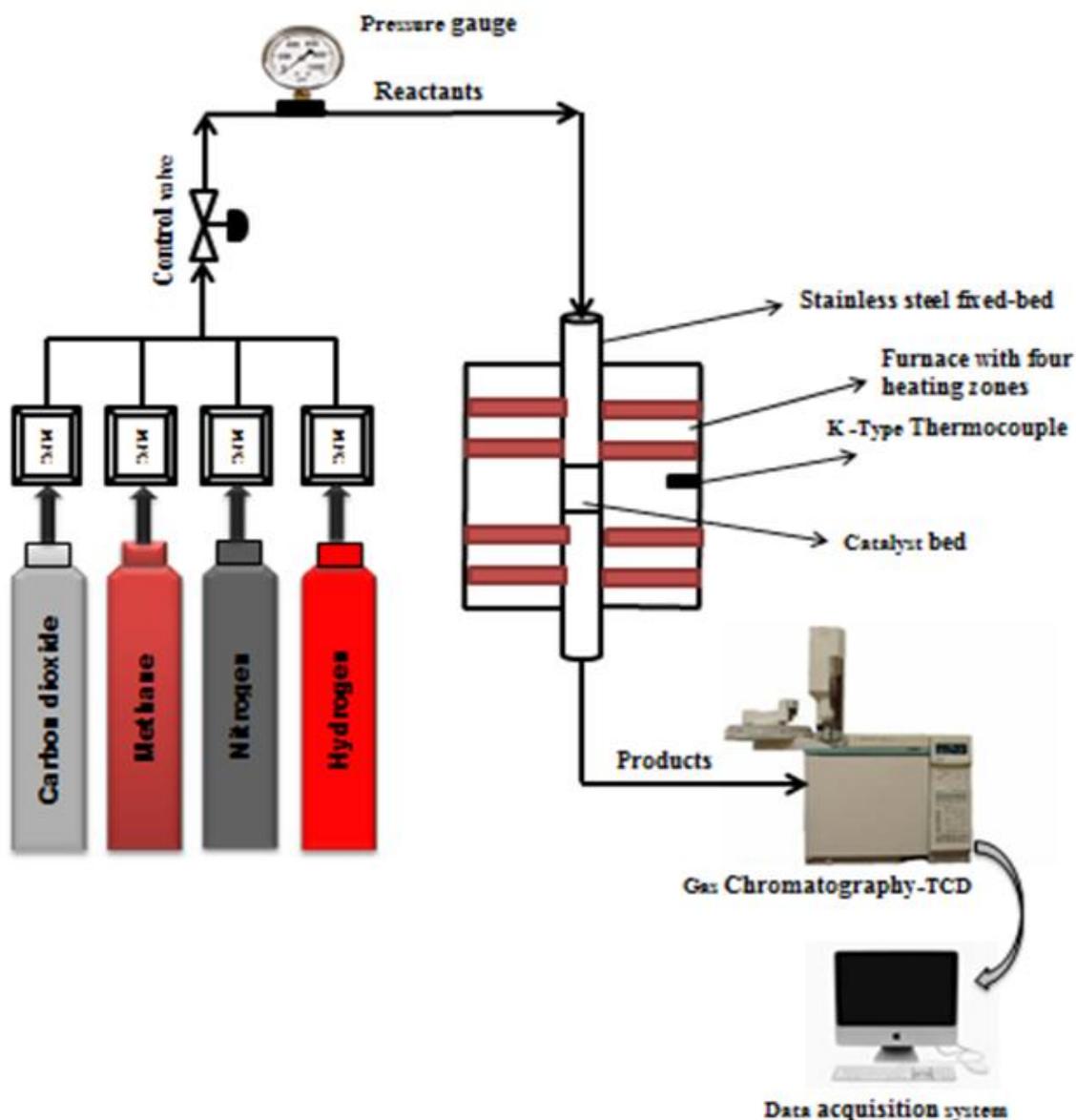
Figure 1. Schematic representation of experimental set up for CO-rich H_2 production from methane dry reforming over Co/CeO_2 catalyst

measurement of the N_2 adsorption-desorption isotherm at 77 K. The pore size distribution and the average pore diameter were determined from desorption section of the isotherm by Barret-Joyner-Halenda (BJH) method. The nature of the chemical bonding of the catalyst was determined by Fourier transform infra-red spectroscopy (FTIR) (Thermo Scientific, Nicolet iS-50). The spectra were obtained using Thermo-Scientific IR spectrometer at room temperature with accumulation of 16 scans at a resolution of 4 cm^{-1}.

2.3. Catalytic activity for Co-rich H_2 production

The experimental set up for CO-rich H_2 production over Co/CeO_2 catalyst is depicted in Figure 1. The methane dry reforming was performed at atmospheric pressure in tubular stainless fixed bed reactor containing 200 mg of the catalysts supported with quartz wool. The tubular fixed bed reactor (internal diameter: 10 mm; Height 35 cm) was placed vertically in a furnace with four heating zones equipped with K-type thermocouple to measure the temperature of the catalyst bed. The catalyst was reduced *in-situ* under the flow of 60 mL/min of H_2/N_2 (ratio 1:5) at 873 K for 1 h. The reactant gases (CO_2 and CH_4) were fed into the fixed bed reactor at feed ratios (CO_2:CH_4) ranged from 0.1 to 1.0. The methane dry reforming was performed at reaction temperatures 923-1023 K. The products and reactants were analyzed by gas chromatography instrument (GC-Agilent 6890 N series) equipped with thermal conductivity detector (TCD). The catalyst performances were evaluated by yields and selectivity defined in Equations (5-8) [4-5].

$$H_2\ Yield\,(\%) = \frac{moles\,of\,H_2\ produced}{2\,moles\,of\,CH_4\ feed} x100\%$$

(5)

$$CO\ yield\,(\%) = \frac{moles\,of\,CO\ produced}{(moles\,of\,CH4 + moles\,of\,CO_2)_{feed}} x100\%$$

(6)

$$Selectivit\,y\ of\ H_2\ (\%) =$$
$$\frac{mole\,of\,H_2}{(moles\,of\,H_2 + total\,moles\,C-containing\ products)_{outlet}} x100\%$$

(7)

$$Selectivity\ of\ CO\,(\%) =$$
$$\frac{mole\,of\,CO}{(moles\,of\,CO + total\,moles\,C-containing\ products)_{outlet}} x100\%$$

(8)

3. Results and Discussion

3.1. Catalysts characterization

The thermal behavior of the catalyst under temperature programmed calcination from 298 to 1173 K is represented by the thermogravimetry (TG) and the differential thermogravimetry (DTG) curves in Figure 2. Significantly, there are four different weight loses represented by peaks I-IV on the DTG curve. The weight changes could be attributed to sequential loss of physical and hydrated water represented by peak I-III and then decomposition of $Co(NO_3)_2$ (Equation (9)) [30].

It is noteworthy that the XRD pattern of the as-synthesized Co/CeO_2 catalyst shows different peaks with varying intensity (cf. Figure 3). The XRD pattern show the existence of CeO_2 with a distinct fluorite-type oxide structure [31]. The diffraction peaks of 28.8º, 31.5º, 33.3º, 37.1º, 45.1º, 47.7º, 56.7º, 59.6º, 65.5º, 69.8º and 77.1º can be ascribed to (111), (220), (200), (311), (400), (220), (311), (222), (440), (400), and (331) of the face-centered cubic (fcc) structure, respectively. Moreover, weak diffraction peak at 2θ of 31.5º, 45.1º, 59.6º, 65.5º, 69.8º and 77.1º can be ascribed to cubic Co_3O_4 crystallites in an unreduced state [32]. The diffraction peaks of CoO or Co could not be detected from the XRD pattern.

The BET measurement of the specific surface area of the catalyst from N_2 adsorption-
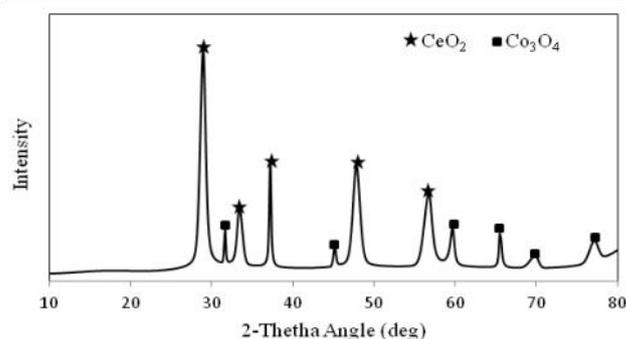
Figure 3. X-ray diffraction patterns of the fresh Co/CeO_2 catalyst

Figure 2. Temperature programmed calcination of the fresh Co/CeO_2 catalyst

desorption isotherms is shown in Figure 4. The Co/CeO_2 catalysts exhibited type-IV isotherm behavior signifying the presence of mesopores in the catalyst sample. The specific surface area of the catalysts was calculated to be 39.89 cm^2/g which is consistent with [26]. The catalysts average pore diameter and the pore volume of 1.157 nm and 0.014 cm^3/g respectively was estimated from the adsorption data using the BJH method.

The FTIR spectra for the Co/CeO_2 catalyst are depicted in Figure 5. Prior to the analysis of the sample, background spectra were collected and subsequently subtracted from the test spectra. This is to ensure that there is no interference with the spectra of the catalysts sample. The bands at 3277, 1489, 658, and 608 cm^{-1} correspond to OH, CO_3^{2-} and metal oxide (M–O), respectively. The tiny bands before 608 cm^{-1} could be attributed to metal oxide (M–O) bonds (Ce–O and Co–O). The presence of OH and CO_3^{2-} could be assigned to water moisture and dissolved atmospheric carbon dioxide.

The FESEM micrographs and EDX dot mapping of the Co/CeO_2 catalyst are depicted in Figure 6. The topographical and elemental information at magnifications 20000× and 80000× of the Co/CeO_2 sample shows that the catalyst particles agglomerated with irregular shapes in large ensembles and have comparatively rough surfaces. The EDX analysis (cf. Figure 6 (c)) shows that the elemental compositions of the catalyst are mainly made up of Co, Ce and O in the right proportions stipulated during the catalyst preparation. The 20 wt% Co obtained from the EDX confirms the efficacy of employing wet-impregnation method for the catalyst preparation.
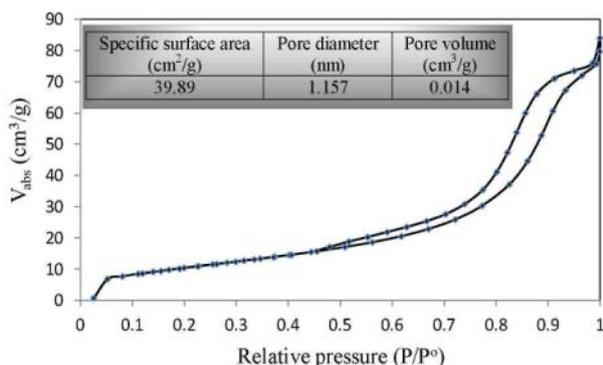
3.2. Catalyst activity

The effects of feed ratios and reaction temperature on the products (H_2 and CO) selectivity are depicted in Figures 7 (a) and (b) respectively. Temperature ranged from 923 to 1023 K was investigated for the methane dry reforming over Co/CeO_2 catalyst. Significantly, the catalyst selectivity for H_2 production increases with feed ratio and temperatures. This trend is consistent with the findings of Xenophon [33] who investigated H_2 production from methane dry reforming over Ni/La_2O_3 catalyst. The Co/CeO_2 catalyst recorded highest H_2 selectivity of 19.56% at unity feed ratio and 1023 K. Thermodynamically, H_2 selectivity is favoured between temperatures ranged 923 to 1023 K. The increase selectivity of the catalyst towards H_2 selectivity is perhaps due to the fact that the Co active site enhances the dissociation of adsorbed CH_4. The selectivity of the Co/CeO_2 catalyst towards CO production is slightly higher compared to that of H_2 (Figure 7(b)). The CO selectivity increases with feed ratio and temperature. The highest CO selectivity of 20.95% at unity feed ratio and temperature of 1023 K was observed for the Co/CeO_2 catalyst. This trend could be as a result of increase in adsorption of CO_2 on the CeO_2 site which gives corresponding CO. Shi *et al*. [34] reported similar trend in their study on methane dry reforming over Ni/Mo_2C catalyst. The authors' findings show that CO_2 activation took place on Mo_2C support site producing CO and O radical.

Hydrogen and CO are desired products of methane dry reforming; hence the catalytic performance in the production process could be evaluated as a function of the product yields. The effects of feed ratios and reaction temperature on H_2 and CO yield are depicted in Figure

Figure 4. BET surface area determination from N_2-physisorption isotherm
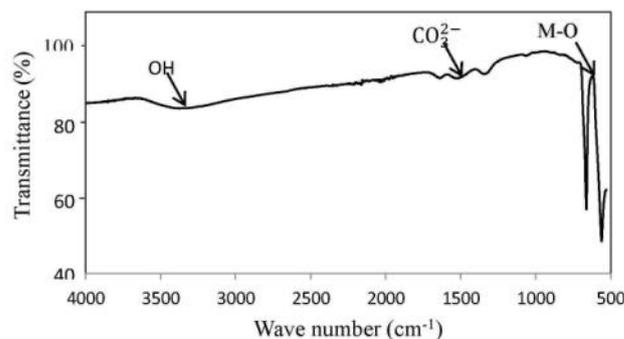
Figure 5. FTIR spectra of the fresh Co/CeO_2 catalyst

8. Significantly, the CO yield increases with feed ratio and temperature (Figure 8(a)). The highest CO yield of 38.05% was obtained at 0.9 feed ratios and 1023 K. It is noteworthy that H_2 yield also increases with feed ratio and temperature. The CeO_2 supported Co catalyst however has a higher activity toward H_2 with yield of 41.98% for at unity feed ratio and 1023 K compared to CO. This trend is in agreement with the work of [35] in their studies on methane dry reforming over MgO promoted Ni–Co/Al_2O_3–ZrO_2 nanocatalyst. However, their findings show a higher yield of CO compared to H_2. This variance could be as result of catalytic performance under different conditions.

The production of synthetic fuels via Fischer-Tropsch process requires syngas ratio >2. Methane dry reforming as an important method for syngas production has the advantages of producing syngas ratio close to unity [22]. The effects of feed ratios and temperature on the syngas yield (H_2 + CO) and syngas ratio (H_2/CO) are depicted in Figure 9. The syngas yield and ratios increase with increase in feed ratio and temperature. The highest syngas yield and ratio of 78.54% and 1.28 were obtained at unity feed ratio and 1023 K. The production of syngas ratio close to unity is favoured at feed ratio equals 0.8 and temperature of 1023 K. The effect of reverse water gas
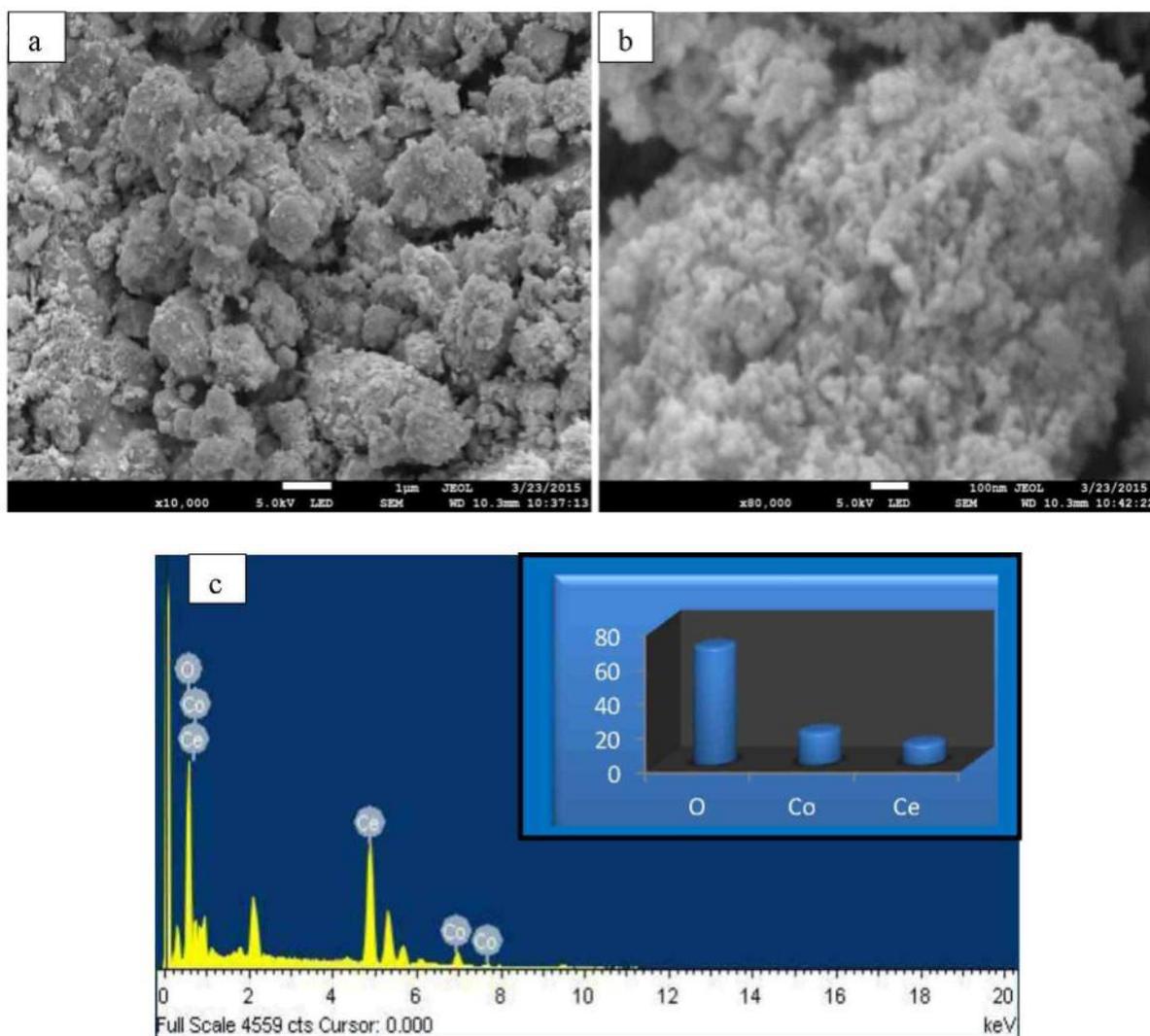
**Figure 6**. FESEM micrographs and EDX spectrum of the Co/CeO_2 catalyst (a) ×10000, (b) ×80000, (c) EDX image
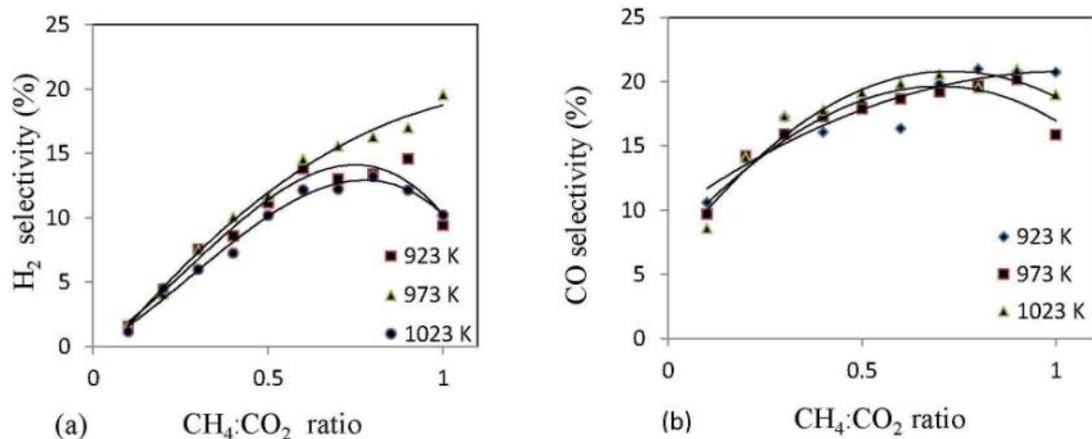
**Figure 7.** Effect of feed ratios and reaction temperature on product selectivity (a) H_2, (b) CO
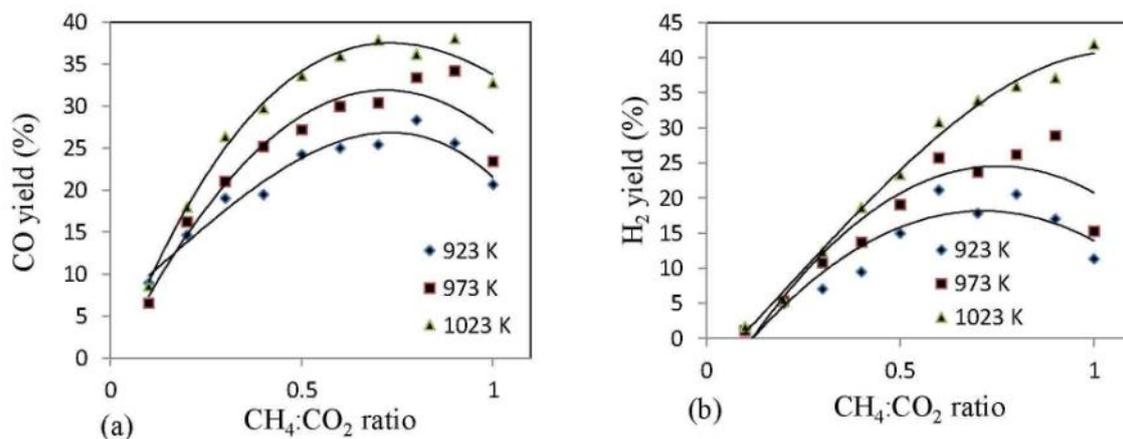
Figure 8. Effects of feed ratios and reaction temperature on product yield (a) H_2, (b) CO
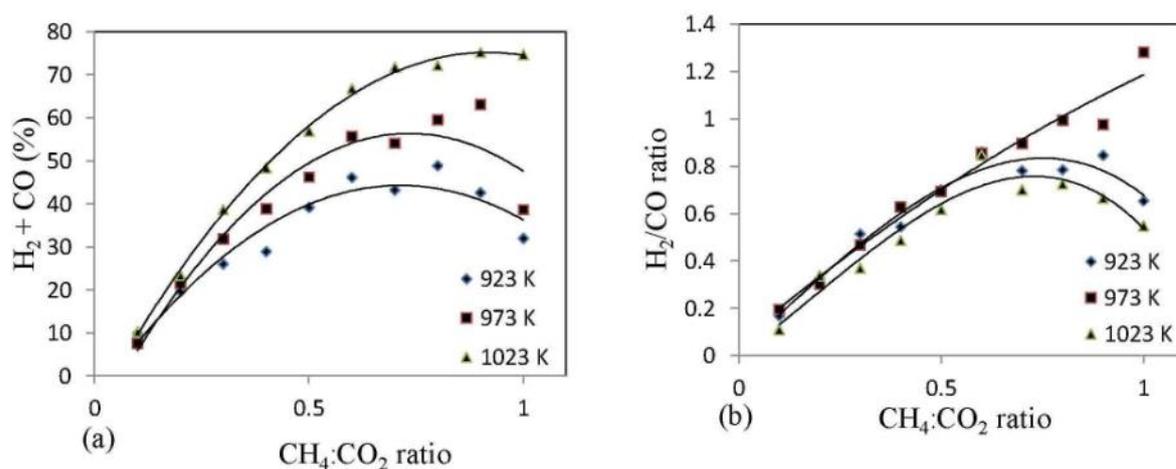

F**igure 9**. Effect of feed ratios and reaction temperature on (a) Syngas yield, (b) Syngas ratio

reaction is noticeable with increase in the feed ratio, hence leads to the reduction in CO yield [36]. Consequentially, the syngas ratio tends to increase above unity. Findings by Serrano-Lotina and Daza [37] shows that production of syngas ratio close to unity is favoured at feed ratio between 0.6 and 0.9. This trend is also corroborated by the work of [38] and [39] who obtained syngas ratio close to unity at feed ratio of 1.

4. Conclusions

In this work, CO-rich hydrogen production via methane dry reforming over Co/CeO_2 catalyst has been investigated. The catalytic performance of the Co/CeO_2 catalyst which was prepared by wet impregnation was studied at reaction temperature ranged 923-1023 K and feed ratios between 0.1-1.0. The catalyst show good activity towards H_2 and CO selectivity and yield with highest H_2 and CO selectivity of 19.56% and 20.95% respectively, while the highest yield of 41.98% and 38.05% were obtained for H_2 and CO respectively. Syngas ratio close to unity was produced, which further confirm the suitability of the methane dry reforming over Co/CeO_2 for the production of syngas for Fischer-Tropsch synthesis. This study has reiterated the potential of Co/CeO_2 which exhibited promising catalytic properties for the production of hydrogen and syngas.

Acknowledgement

References

[1]   Ursua, A. (2012). Hydrogen production from water Electrolysis : Current Status and Future Trends: in *Proceedings of the IEEE*, 100 (2): 410-426.

[2]   Kirtay, E. (2011). Recent advances in production of hydrogen from biomass. *Energy Convers. Manag.,* 52 (4): 1778-1789.

[3]   Balat, H., Kirtay, E. (2010). Hydrogen from biomass - Present scenario and future prospects. *Int. J. Hydrogen Energy*, 35 (14): 7416-7426.

[4]   Balat, M., Balat, M. (2009). Political, economic and environmental impacts of biomass-based hydrogen. *Int. J. Hydrogen Energy*, 34 (9): 3589-3603.

[5]   Mekhilef, S., Saidur, R., Safari, A. (2012). Comparative study of different fuel cell technologies. *Renew. Sustain. Energy Rev.*, 16(1): 981-989.

[6]   Kirubakaran, A., Jain, S., Nema, R.K. (2009). A review on fuel cell technologies and power electronic interface. *Renew. Sustain. Energy Rev.*, 13 (9): 2430-2440

[7]   Arora, K. (2014). International journal of Emerging Trends in Science and Technology. *Int. J. Emerg. Trends Sci. Technol.*, 1(10): 1691-1698.

[8]   Sharaf, O.Z., Orhan, M.F. (2014). An overview of fuel cell technology: Fundamentals and application. *Renew. Sustain. Energy Rev.*, 32: 810-853.

[9]   Xiong, H., Moyo, M., Motchelaho, M.A., Tetana, Z.N., Dube, S.M.A., Jewell, L.L., Coville, N.J. (2014). Fischer-Tropsch synthesis: Iron catalysts supported on N-doped carbon spheres prepared by chemical vapor deposition and hydrothermal approaches. *J. Catal.*, 311: 80-87.

[10]   Gabriel, K.J., Noureldin, M., El-Halwagi, M.M., Linke, P., Jiménez-Gutiérrez, A., Martínez, D.Y. (2014). Gas-to-liquid (GTL) technology: Targets for process design and water-energy nexus. *Curr. Opin. Chem. Eng.*, 5: 49-54.

[11]   Aasberg-Petersen, K., Dybkjær, I., Ovesen, C.V., Schjødt, N.C., Sehested, J., Thomsen, S.G. (2011). Natural gas to synthesis gas - Catalysts and catalytic processes. *J. Nat. Gas Sci. Eng.*, 3 (2): 423-459.

[12]   Li, K., Zhang, R., Bi, J. (2010). Experimental study on syngas production by co-gasification of coal and biomass in a fluidized bed. *Int. J. Hydrogen Energy*, 35(7): 2722–2726.

[13]   Wu, T.Y., Mohammad, A.W. (2007). Palm oil mill effluent (POME) treatment and bioresources recovery using ultrafiltration membrane: effect of pressure on membrane fouling *Biochem. Eng. J.*, 35(3): 309-317.

[14]   Yoshiie, R., Taya, Y., Ichiyanagi, T., Ueki, Y., Naruse, I. (2013). Emissions of particles and trace elements from coal gasification. *Fuel*, 108: 67-72.

[15]   Man, Y., Yang, S., Xiang, D., Li, X., Qian, Y. (2014). Environmental impact and techno-economic analysis of the coal gasification process with/without CO_2 capture. *J. Clean. Prod.*, 71: 59-66.

[16] Bhandari, R., Trudewind, C. A., Zapp, P. (2014). Life cycle assessment of hydrogen production via electrolysis: a review. *J. Clean. Prod.*, 85: 151-163.

[17] Koh, A., Chen, L., Keeleong, W., Johnson, B., Khimyak, T., Lin, J. (2007). Hydrogen or synthesis gas production via the partial oxidation of methane over supported nickel–cobalt catalysts. *Int. J. Hydrogen Energy*, 32(6): 725-730.

[18] Kothari, R., Buddhi, D., Sawhney, R.L. (2008). Comparison of environmental and economic aspects of various hydrogen production methods. *Renew. Sustain. Energy Journal,* 12(2): 553-563

[19] Sehested, J. (2006). Four challenges for nickel steam-reforming catalysts *Catal. Today*, 111 (1-2): 103-110.

[20] Braga, T.P., Santos, R.C.R., Sales, B.M.C., da Silva, B.R., Pinheiro, A.N., Leite, E.R., Valentini, A. (2014). CO_2 mitigation by carbon nanotube formation during dry reforming of methane analyzed by factorial design combined with response surface methodology," *Chinese J. Catal.*, 35 (4): 514-523.

[21] Whitemore, N.W. (2007). Greenhouse gas catalytic reforming to syngas. Columbia University in the City of New York.

[22] Budiman, A.W., Song, S.H., Chang, T.S., Shin, C.H., Choi, M.J. (2012). Dry Reforming of Methane Over Cobalt Catalysts: A Literature Review of Catalyst Development. *Catal. Surv. from Asia*, 16(4): 183-197.

[23] Ruckenstein, E., Wang, H.Y. (2002). Carbon Deposition and Catalytic Deactivation during CO_2 Reforming of CH_4 over Co/γ-Al_2O_3 Catalysts, *J. Catal.*, 205(2): 289-293.

[24] Lavoie, J.M. (2014). Review on dry reforming of methane, a potentially more environmentally-friendly approach to the increasing natural gas exploitation, *Front. Chem.*, 2: 1-17.

[25] Luisetto, I., Tuti, S., Di Bartolomeo, E. (2012). Co and Ni supported on CeO_2 as selective bimetallic catalyst for dry reforming of methane. *Int. J. Hydrogen Energy*, 37: 15992-15999.

[26] Abasaeed, A.E., Al-fatesh, A.S., Naeem, M.A., Ibrahim, A.A., Fakeeha, A.H. (2015) Catalytic performance of CeO_2 and ZrO_2 supported Co catalysts for hydrogen production via dry reforming of methane, *Int. Hydrog. Energy*, 40: 6818-6826.

[27] Lee, S.S., Zhu, H., Contreras, E.Q. Prakash, A., Puppala, H.L., Colvin, V.L. (2012). High temperature decomposition of cerium precursors to form ceria nanocrystal libraries for biological applications, *Chem. Mater.* 24: 424-432.

[28] Djaidja, A., Libs, S., Kiennemann, A., Barama, A. (2006). Characterization and activity in dry reforming of methane on NiMg/Al and Ni/MgO catalysts, *Catal. Today*, 113(3-4): 194-200.

[29] Abd. El-Hafiz, D.R., Ebiad, M.A., El-salamony, R.A. (2014). Hydrogen selectivity and carbon behavior during gasoline steam reforming over nano-Al_2O_3 catalysts. *Mater. Renew. Sustain. Energy*, 3(3): 1-13.

[30] Foo, S.Y., Cheng, C.K., Nguyen, T.H., Adesina, A.A. (2011). Kinetic study of methane CO_2 reforming on Co-Ni/Al_2O_3 and Ce-Co-Ni/Al_2O_3 catalysts. *Catal. Today*, 164(1): 221-226.

[31] Du, X., Zhang, D., Shi, L., Gao, R., Zhang, J. (2012). Morphology Dependence of Catalytic Properties of Ni/CeO_2 Nanostructures for Carbon Dioxide Reforming of Methane. *J. Phys. Chem.*, 1: 10009-10016.

[32] Da Silva, A.M., De Souza, K.R., Mattos, L.V., Jacobs, G., Davis, B.H., Noronha, F.B. (2011). The effect of support reducibility on the stability of Co/CeO_2 for the oxidative steam reforming of ethanol, *Catal. Today*, 164: 234-239.

[33] Verykios, X.E. (2003). Catalytic dry reforming of natural gas for the production of chemicals and hydrogen. *Int. J. Hydrogen Energy*, 28(10): 1045-1063.

[34] Shi, C., Zhang, A., Li, X., Zhang, S., Zhu, A., Ma, Y., Au, C. (2012). Ni-modified Mo_2C catalysts for methane dry reforming, *Appl. Catal. A Gen.*, 432: 164-170.

[35] Sajjadi, S. M., Haghighi, M., Rahmani, F. (2014). Dry reforming of greenhouse gases CH_4/CO_2 over MgO-promoted Ni-Co/Al_2O_3-ZrO_2 nanocatalyst: effect of MgO addition via sol-gel method on catalytic properties and hydrogen yield. *J. Sol-Gel Sci. Technol.* 70: 111-114

[36] Rahemi, N., Haghighi, M., Babaluo, A.A., Allahyari, S., Jafari, M.F. (....) Syngas production from reforming of greenhouse gases CH_4/CO_2 over Ni-Cu/Al_2O_3 nanocatalyst: Impregnated vs. plasma-treated catalyst, *Energy Convers. Manag.*, 84: 50-59.

[37] Serrano-Lotina, A., Daza, L. (2014). Influence of the operating parameters over dry reforming of methane to syngas. *Int. J. Hydrogen Energy*, 39(8): 4089-4094.

[38] Sharifi, M., Haghighi, M., Rahmani, F., Karimipour, S. (2014). Syngas production via dry reforming of CH_4 over Co- and Cu-promoted Ni/Al_2O_3-ZrO_2 nanocatalysts synthesized via sequential impregnation and sol–gel methods. *J. Nat. Gas Sci. Eng.*, 21: 993-1004.

[39] Nematollahi, B., Rezaei, M., Khajenoori, M. (2011). Combined dry reforming and partial oxidation of methane to synthesis gas on noble metal catalysts. *Int. J. Hydrogen Energy*, 36 (4): 2969-2978.